Percentage Depth Dose in Potential Wood-based Phantom Materials Using Monte Carlo Geant4 Application for Emission Tomography with a 6MV Photon Beam

Siti Hajar Zuber [a,*] Muhammad Fahmi Rizal Abdul Hadi,[b] Nurul Ab. Aziz Hashikin,[b] Mohd Fahmi Mohd Yusof,[c] Muhammad Safwan Ahmad Fadzil,[a] and Mohd Zahri Abdul Aziz [d]

* *Corresponding author: hajarzuber@ukm.edu.my*

DOI: 10.15376/biores.20.4.10858-10871

GRAPHICAL ABSTRACT

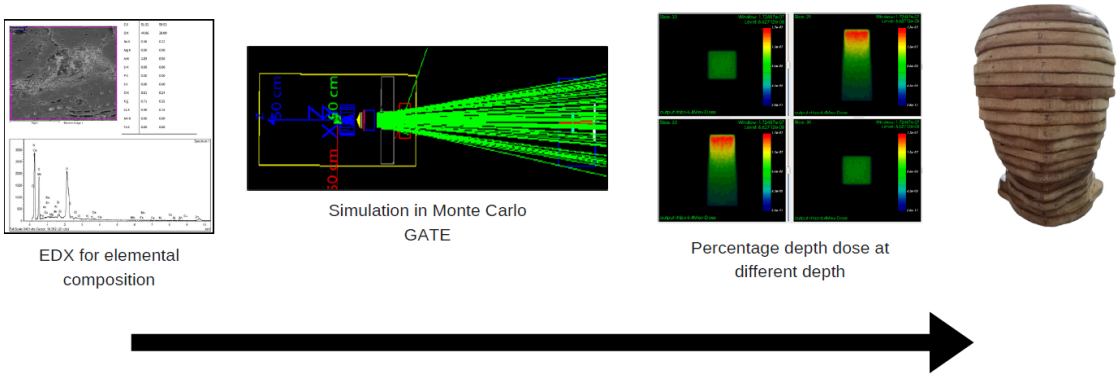

Percentage Depth Dose in Potential Wood-based Phantom Materials Using Monte Carlo Geant4 Application for Emission Tomography with a 6MV Photon Beam

Siti Hajar Zuber [a,*] Muhammad Fahmi Rizal Abdul Hadi,[b] Nurul Ab. Aziz Hashikin,[b] Mohd Fahmi Mohd Yusof,[c] Muhammad Safwan Ahmad Fadzil,[a] and Mohd Zahri Abdul Aziz [d]

The percentage depth doses of various wood-based phantom materials were evaluated using Monte Carlo GATE simulation at 6MV photon beam. Several elemental compositions of phantom materials developed over the years were collected retrospectively, and the data were used to build each phantoms' specific geometries and compositions in a Monte Carlo GATE algorithm. Upon the construction of the linear accelerator in GATE, the percentage depth doses were measured for each of the phantom materials, and results were recorded accordingly. The output revealed that all of the samples pass the 3 %/2 mm comparison by gamma index at 96.8%. The findings of this work supported the potential of wood-based phantom material in radiotherapy and medical physics application.

DOI: 10.15376/biores.20.4.10858-10871

Keywords: Monte Carlo simulation; GATE; Percentage depth dose; Phantom material; Wood-based

*Contact information: a: Center for Diagnostic, Therapeutic and Investigative Studies, Faculty of Health Sciences, Universiti Kebangsaan Malaysia, 50300, Kuala Lumpur, Malaysia; b: School of Physics, Universiti Sains Malaysia, 11800, Penang, Malaysia; c: Faculty of Nursing and Health Sciences, Universiti Islam Melaka, 78200 Alor Gajah, Malacca; d: Pusat Perubatan USM, Universiti Sains Malaysia, 13200, Penang, Malaysia; * Corresponding author: hajarzuber@ukm.edu.my*

INTRODUCTION

A phantom is often recognised as a model that closely resembles the human body and its anatomy (Jusufbegović *et al.* 2023). It may be composed of media with close equivalents to human soft tissue (Breslin *et al.* 2023) in terms of size, shape, location, density, and radiation interaction with matter. Dosimetric phantoms are model phantoms developed to quantify and evaluate organ doses following irradiation, either internally or externally, in response to the evolution of computational phantoms. In photon radiation applications, such as diagnostic imaging and radiotherapy, phantoms are essential for accurately assessing dose distribution, attenuation characteristics, and energy deposition within biological tissues (Aitelcadi *et al.* 2020; Breslin *et al*. 2023; Kairn *et al.* 2023; Lin *et al.* 2025). The need to replicate the human body and its characteristics in radiation studies has led researchers to explore various wood-based materials as phantoms, which are deemed adequate based on physico-mechanical properties, attenuation, and scattering investigations.

Characterising the phantom is essential for creating a model that closely mimics a real human body, particularly regarding its attenuation and radiation properties. To produce

a comparable phantom, it is necessary to analyse its properties to ensure its suitability as a material for radiation studies. *Rhizophora* wood has gained significant attention as a phantom material due to its close compatibility with soft tissue, offering its potential as phantom in radiation dosimetry. This makes it suitable for simulating human-equivalent attenuation and scattering characteristics in photon-based simulations. Additionally, the fine and homogeneous grain structure of *Rhizophora* minimises internal voids and density fluctuations, which are often problematic in other natural wood types and can introduce dose inhomogeneities during irradiation. *Rhizophora* is also widely available and sustainable, as it is cultivated in managed mangrove forests across tropical regions, allowing for reproducible sourcing and consistent material quality which is an important factor in phantom construction. Previous literature reported the potential of *Rhizophora* based phantom material based on its physical and mechanical properties, effective atomic number and attenuation properties (Bradley *et al*. 1991; Abuarra *et al.* 2014; binti Zuber *et al.* 2024).

Dosimetry quality assurance in radiotherapy is vital in ensuring that the dose delivery during the treatment is precise and accurate. The International Atomic Energy Agency (IAEA) recommended a primary standard in the measurement of absorbed dose in radiotherapy setting (IAEA 2000), to reduce the uncertainties in the dosimetry of the radiotherapy beams and at the same time, to ensure that each patient received appropriate exposure to radiation and minimise any unnecessary and unwanted radiation to healthy tissues. In radiotherapy, water is the reference medium for measurements of absorbed dose following recommendations of most dosimetry protocols such as TRS-398 from IAEA or TG-51 from AAPM.

It is impossible to determine the radiation dose received by patients directly; thus, there is a need for phantom material to replace human body in radiotherapy (Yadav *et al.* 2023). Previous research studies often reported the potential of various phantom materials in mimicking the properties of human soft tissues; however, the materials that have been employed are not without several disadvantages. Widely commercialised plastic-based phantoms, such as acrylic phantoms, are reported to have disparities, especially in elemental composition, with an earlier study reported the inability of these phantoms to closely mimic the human soft tissues (Yohannes *et al.* 2012), besides having incomparable dosimetric properties at different energy ranges. The disparities in elemental composition also have been further complicated, as some solid equivalent materials were given similar names but differ in the mixes and formulation (Allahverdi *et al.* 1999).

A Monte Carlo algorithm is one of the most established open-source codes, most often used in the simulation of radiation-based analyses including nuclear medicine and radiotherapy. It often has been previously employed in a wide range of investigations and applications, and since then, adjustments have been made to the toolkit to satisfy the needs of various user populations. GATE, or the Geant4 Application for Emission Tomography, is a nuclear medicine-specific modular, adaptable, programmable simulation toolset (Jan *et al.* 2011, 2004; Sarrut *et al.* 2022). GATE now has various laboratories committed to enhancing, documenting, and exhaustively testing GATE against the majority of commercially available imaging systems.

In this work, the percentage depth dose of various plastic and wood-based phantom materials, including solid water, polystyrene, polymethyl methacrylate (PMMA), plastic water, and virtual water were measured in Monte Carlo GATE simulation and gamma indexes were calculated. In addition, the investigation was also extended to assess the dosimetric performance of binderless and adhesive-enhanced wood-based phantoms,

including those formulated with materials such as soy protein isolate (SPI) and crosslinking agents like itaconic acid polyamidoamine-epichlorohydrin (IA-PAE), soy-lignin, corn starch, and tannin. The innovative aspect of this work lies in the investigation of sustainable and biodegradable wood-derived materials formulated with components such as soy protein isolate (SPI), lignin, corn starch, tannin, and crosslinking agents including itaconic acid polyamidoamine-epichlorohydrin (IA-PAE) as potential alternatives to conventional tissue-equivalent phantoms, through a simulation-based approach.

EXPERIMENTAL

Collection of Elemental Composition of Various Phantom Materials

Elemental compositions of potential phantom materials were collected retrospectively from previous investigations by other researchers. In this work, all the composition fractions were documented in percentage value for use in Monte Carlo GATE simulation. Table 2 summarizes the elemental composition collected in previous investigations (Seco and Evans 2006; Borcia and Mihailescu 2007; Taylor *et al.* 2007; Yusof *et al.* 2017; Abd Hamid *et al.* 2018; Zuber *et al.* 2021a; Samson *et al.* 2023).

Monte Carlo Toolkit: GATE for the Simulation

The computer model used in this investigation was a Lenovo H30-50 running the Linux Mint 19 Tara 64-bit operating system (OS).

In the simulation, the GATE v9.0 with geant4 v10.06.p03 and Root v6.24/0 platform was employed. For this work, the SPECTHead example was changed, and the GATE input file simulated the experimental configuration by utilising macro files with a range of commands. In this work, a list of 20 item checklist – RECORDS – Reporting of Monte Carlo Radiation Transport Studies – was reported, in an effort to refine the quality of Monte Carlo investigation as proposed by AAPM Research Committee Task Group 268 (Sechopoulos *et al.* 2018). Table 1 reports the RECORDS checklist.

Table 1. RECORDS Checklist for Monte Carlo GATE Simulation

Checklist item #	Item name	Description
2, 3	Code, version/release date	GATE v9.0 with geant4 v10.06.p03 and Root v6.24/0 platform Release Date: 03/02/2020
4, 17	Validation	Code was being validated against experimental measurements (Linear accelerator configuration for percentage depth dose measurement based on Elekta Synergy Agility LINAC (Elekta Medical Systems, Crawley, UK)
5	Timing/system configuration	CPU based simulation: 3.9 GHz and 32 threads CPU CPU/GPU model number: Intel Xeon Gold 6242 NVIDIA Quadro P2200
8	Source description	Source of phase-space: Energy spectrum from interaction gamma radiation; electron beam with energy of 6.4 MeV was simulated with 10^8 histories and photon spectrum produced were recorded in ROOT file Phasespace. Phasespace volume was located before the multileaf collimator. The Phasespace contains photon spectrum were then simulated to get the percentage depth dose with the history of 2×10^9
9	Cross-sections	Cross-section data: Livermore model
10	Transport parameters	EM Standard Option 3 (geant4); with electron cut-off of 1.0 mm and photon cut-off of 0.1 mm at material phantom and default 1.0 mm for others
11	VRT and/or AEIT	Bremsstrahlung Splitting with active splitting of 100
12	Scored quantities	DoseActor
13, 18	# histories/statistical uncertainty	Histories for electron beam to generate PhaseSpace = 1×10^8 while for photon PhaseSpace is 2×10^9; Voxel size for dose image is 5 × 5 × 5 mm with size of image is 30 × 30 × 30 cm
14	Statistical methods	Gamma index
15, 16	Postprocessing	Nil

PDD: Percentage depth dose, GPU: Graphics processing unit, CPU: Central processing unit, VRT: Variance reduction techniques, AEIT: Approximate efficiency improving techniques

Table 2. Summary of the Elemental Composition Collected in Previous Investigations

Code	Sample	H	C	N	O	Cl	Ca	Br	F	Na	Mg	P	S	K	Mn	Fe
B	Solid water[a]	8.09	67.22	2.40	19.84	0.13	2.32									
C	Polystyrene[a]	7.74	92.26													
D	PMMA[a]	8.05	59.98		31.96											
E	Plastic water[a]	9.25	62.82	1.00	17.94	0.96	7.95	0.03								
F	Virtual water[b]	7.70	68.74	2.27	18.86	0.13	2.31									
G	Binderless *Rhizophora*[c]		48.42	3.15	48.43											
H	6% soy-lignin *Rhizophora*[c]		47.35	4.06	48.59											
I	12% soy-lignin *Rhizophora*[c]		47.74	3.09	49.17											
L	Corn starch *Rhizophora*[e]		27.20	0.25	72.55											
M	SPI0[f]		51.05	2.01	46.88								0.06			
N	SPI5[f]		51.81	4.89	41.50	0.25	0.64			0.33	0.05		0.11	0.09		0.22
O	SPI10[f]		52.07	3.09	43.32	0.11	1.00			0.30						0.20
P	SPI15[f]		56.34	1.07	40.11	0.26	1.09			0.45	0.06	0.04	0.10	0.10	0.08	0.30
Q	SPI20[f]		53.99	1.96	42.15	0.20	1.00			0.36		0.01	0.05		0.03	0.25
R	Tannin-added *Rhizophora*[g]		51.25		43.11				5.64							

Note: Data from Seco and Evans (2006), Borcia and Mihailescu (2007), Taylor *et al.* (2007), Yusof *et al.* (2017), Abd Hamid *et al.* (2018), Zuber *et al.* (2021a), and Samson *et al.* (2023). SPI0 = untreated *Rhizophora* spp., SPI5 = SPI/NaOH/IA-PAE/*Rhizophora* spp., SPI10 = SPI/NaOH/IA-PAE/*Rhizophora* spp., SPI15 = SPI/NaOH/IA-PAE/R*hizophora* spp., and SPI20 = SPI/NaOH/IA-PAE/*Rhizophora* spp. indicate 0, 5, 10, 15, and 20 wt% IA-PAE.

To ensure reproducibility and transparency, all assumptions made in this Monte Carlo GATE simulation are summarised in Table 3.

Table 3. List of Assumptions Made in Monte Carlo GATE Simulation

Assumption	Description
Material homogeneity	Each phantom material was assumed to be compositionally uniform
Elemental composition	Elemental compositions were normalised to 100% by weight
Density uniformity	Bulk densities of all materials were applied uniformly throughout the phantom volume
Geometry and dimensions	All phantoms were modeled as slabs of identical size (e.g., 30 × 30 × 30 cm^3)
Beam quality	A 6 MV photon beam was simulated using validated phase-space data from a modeled linear accelerator
Statistical uncertainty	The number of particle histories (2 × 10^9) was selected to ensure <1% statistical uncertainty in PDD results
Dose scoring medium	Dose was scored in water-equivalent voxelised detectors within the phantom

In this simulation, the output was read in ROOT graphical user interface TBrowser. Lateral dose profile was visualised in vv 4D Slicer (Rit *et al.* 2011), and predetermined points were marked and labelled with *P1* and *P2* in the image to obtain the intensity value with increasing depth. Fig. 1 illustrates the example of lateral dose profile obtained from vv 4D Slicer.

The gamma index comparison was performed, and output with 100% of the points passing the dose difference/distance to agreement comparison will demonstrate that all points passed the comparison. In this work, 3%/2 mm gamma index comparison was evaluated and recorded accordingly.

Each phantom material was designed in the simulation to mimic a standard solid water phantom at a dimension of (30 × 30 × 30) cm. Figure 2 provides a two-dimensional bird's eye view of the geometry in GATE simulation. Linear accelerator (ELEKTA Synergy) in Pusat Perubatan, Universiti Sains Malaysia, Bertam was modelled in the GATE simulation. 6 MV photon energy was used in this work at the field size of (10 × 10) cm, without bolus and multileaf collimator (MLC). The setup was simulated via GATE (version 1.2.3) MC package, with histories of 1×10^8. After the launch of ROOT for output, the simulation data revealed results in the form of entries for the chosen energy window, and the percentage depth dose was recorded at each depth. Figure 3 illustrates the GATE file before simulation specifically to produce an energy spectrum equivalent to a 6 MV photon energy.

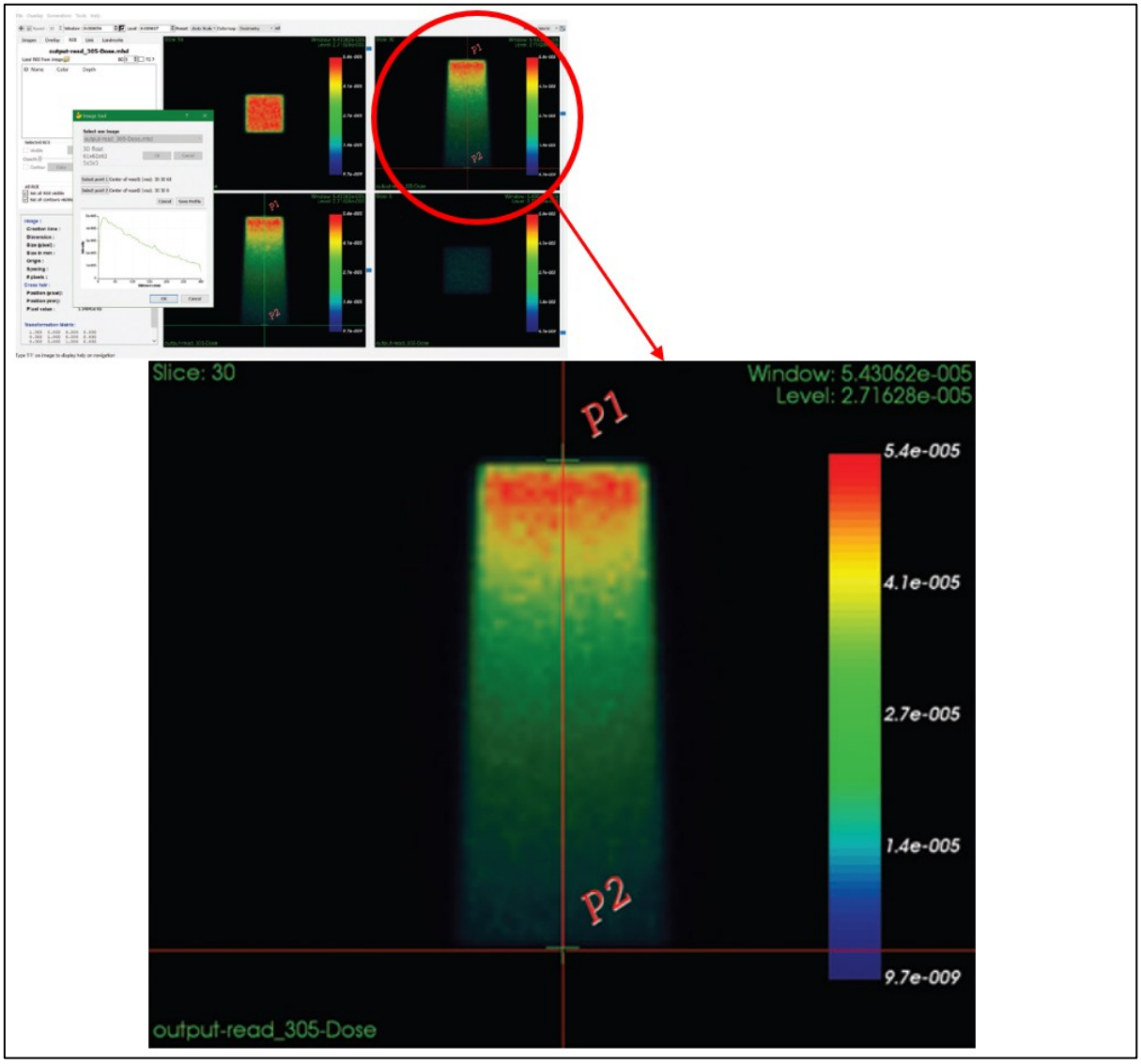

Fig. 1. Gamma index analysis measured using the lateral dose profile illustrated in vv 4D Slicer

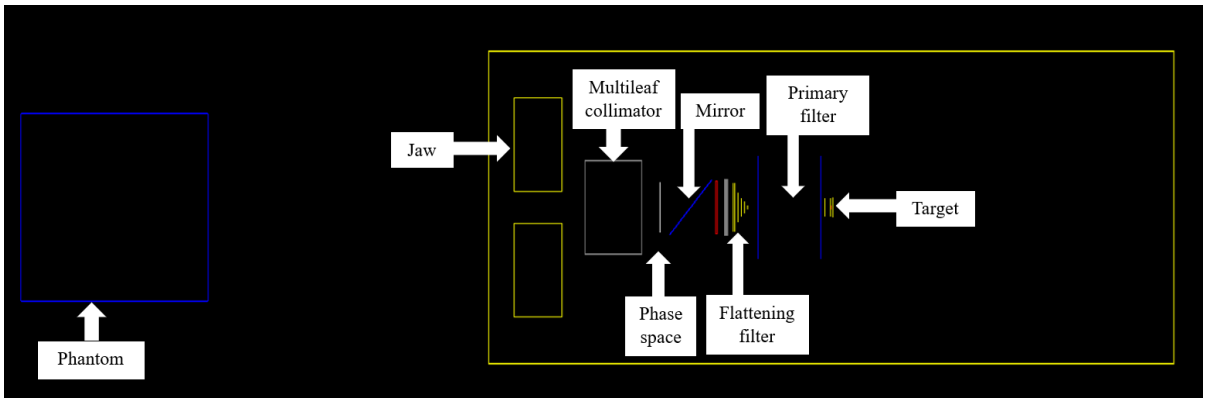

Fig. 2. Two-dimensional bird's eye view (BEV) of the geometry for GATE simulation

1

```
#=====================================================
# VERBOSITY
#=====================================================

/control/execute mac/verbose.mac

#=====================================================
# VISUALISATION
#=====================================================

#/control/execute mac/visu.mac

# =====================================================
# GEOMETRY
# =====================================================

/gate/geometry/setMaterialDatabase data/GateMaterials.db

# WORLD
/gate/world/setMaterial           Air
/gate/world/geometry/setXLength   1 m
/gate/world/geometry/setYLength   1 m
/gate/world/geometry/setZLength   2.8 m
/gate/world/vis/setVisible 1
/gate/world/vis/forceWireframe

# LINAC HEAD
# World origin is in the center of the beam e- source (not the real
# isocenter of the gantry room)
/gate/geometry/setMaterialDatabase data/LinacMaterials.db
/control/execute mac/linac_head.mac

# WATER BOX
/gate/world/daughters/name              waterbox
/gate/world/daughters/insert            box
/gate/waterbox/setMaterial              Rhizo
/gate/waterbox/placement/setTranslation 0 0 -1150 mm
/gate/waterbox/geometry/setXLength      300 mm
/gate/waterbox/geometry/setYLength      300 mm
/gate/waterbox/geometry/setZLength      300 mm
/gate/waterbox/vis/setColor             blue

# VIRTUAL PLANE FOR PHASE SPACE
/gate/linac/daughters/name               PhS_Plane
/gate/linac/daughters/insert             cylinder
/gate/PhS_Plane/setMaterial              Vacuum
/gate/PhS_Plane/geometry/setRmin         0 mm
/gate/PhS_Plane/geometry/setRmax         40 mm
/gate/PhS_Plane/geometry/setHeight       1 nm
/gate/PhS_Plane/placement/setTranslation 0.0 0.0 -275 mm
/gate/PhS_Plane/vis/setColor             white
/gate/PhS_Plane/vis/setVisible           1
```

2

```
# =====================================================
# PHYSICS
# =====================================================

/gate/physics/addPhysicsList emstandard_opt4

/gate/physics/Gamma/SetCutInRegion      world 1 mm
/gate/physics/Electron/SetCutInRegion   world 1 mm
/gate/physics/Positron/SetCutInRegion   world 1 mm

/gate/physics/Gamma/SetCutInRegion      waterbox 0.5 mm
/gate/physics/Electron/SetCutInRegion   waterbox 0.5 mm
/gate/physics/Positron/SetCutInRegion   waterbox 0.5 mm

#=====================================================
# DETECTORS
#=====================================================

# -----------------------------------------------------
# Kill actor to stop particles when they go inside a region

/gate/actor/addActor          KillActor killer0
/gate/actor/killer0/attachTo  kill_box_top
/gate/actor/addActor          KillActor killer1
/gate/actor/killer1/attachTo  kill_box_bottom
/gate/actor/addActor          KillActor killer2
/gate/actor/killer2/attachTo  kill_box_bottom2

# -----------------------------------------------------
# the following actor regularly store the current number of
# event/track/step in a file

/gate/actor/addActor               SimulationStatisticActor stat
/gate/actor/stat/save              output/output-rhizo-6.4Mev.txt
/gate/actor/stat/saveEveryNSeconds 10

# -----------------------------------------------------
# the following actor stores 3D Dose/Edep distributions

/gate/actor/addActor                                DoseActor  doseDistribution
/gate/actor/doseDistribution/attachTo                  waterbox
/gate/actor/doseDistribution/stepHitType            random
/gate/actor/doseDistribution/setPosition            0 0 0 mm
/gate/actor/doseDistribution/setVoxelSize           5 5 5 mm
/gate/actor/doseDistribution/setSize               305 305 305 mm
#/gate/actor/doseDistribution/saveEveryNSeconds     20
/gate/actor/doseDistribution/enableEdep             false
/gate/actor/doseDistribution/enableUncertaintyDose true
/gate/actor/doseDistribution/enableDose             true
/gate/actor/doseDistribution/enableNumberOfHits     false
/gate/actor/doseDistribution/save                   output/output-rhizo-6.4Mev.mhd
#/gate/actor/doseDistribution/normaliseDoseToIntegral   true
```

3

```
#=====================================================
# INITIALISATION
#=====================================================

/gate/run/initialize

#=====================================================
# BEAMS
#=====================================================

# Read from Phase Space files. Here we indicate the type of particle
# (gamma) because this information is not stored in the PhS to gain
# space. Moreover, we set 'useRandomSymmetry' to generate more
# particle than the number of particle in the PhS, using a Z axis
# symmetry.

/gate/source/addSource                          beam_g phaseSpace
/gate/source/beam_g/addPhaseSpaceFile           output/output-PhS-6.4_0.1_Mev.root
/gate/source/beam_g/setParticleType             gamma
/gate/source/beam_g/attachTo                    PhS_Plane
/gate/source/beam_g/useRandomSymmetry           true


#=====================================================
# START BEAMS
#=====================================================

/gate/random/setEngineName MersenneTwister
/gate/random/setEngineSeed auto
/gate/application/noGlobalOutput

#/tracking/verbose 2

/gate/application/setTotalNumberOfPrimaries 2e9
/gate/application/start
```

Fig. 3. GATE input file for energy spectrum before percentage depth dose simulation

RESULTS AND DISCUSSION

Most of the phantom materials developed over the years were mentioned and cited in previous literature summarising the evolution of *Rhizophora*-based phantom (Zuber *et*

al. 2021b). Thus, the published work inspired the current investigation, to demonstrate its feasibility for radiation study especially in terms of percentage depth dose. Based on the result, all the phantom materials demonstrated 100% dose at 1.5 cm depth, adhering to the depth at maximum dose for 6 MV energy. Figure 4 shows the percentage depth doses of various plastic and wood-based phantoms.

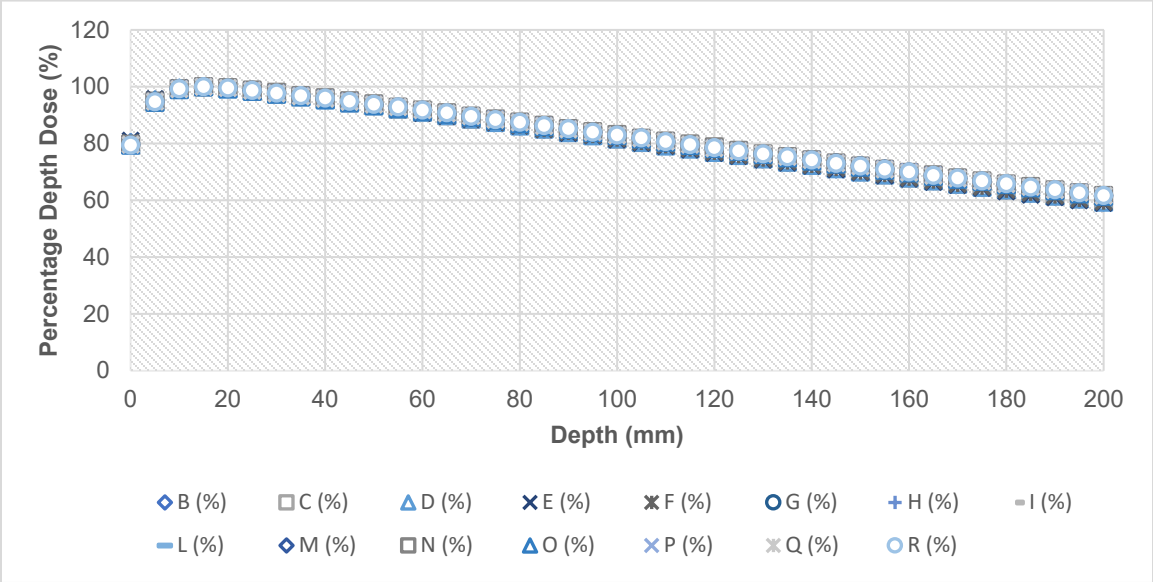

Fig. 4. The percentage depth doses of various plastic and wood-based phantoms

The output curve is in agreement with the percentage depth dose curve for 6 MV photon energy, with build-up region accounting for the secondary charged particles with relatively long ranges that interact with photons inside the phantom, such as in the photoelectric effect, Compton effect, and pair production. Owing to the continuously decreasing energy fluence of the photons, the percentage depth dose decreases with depth beyond $d_{max.}$

The proportion of point dose passing the gamma criteria, known as gamma index, was calculated for every phantom material. The gamma index percentage comparison is demonstrated in Table 4. All the samples achieved the gamma index comparison with water in which 100% of the points pass the 3%/2 mm comparison, except for samples G, H, M, N and P (binderless *Rhizophora*, 6% soy-lignin *Rhizophora*, SPI0, SPI5 and SPI15) at 96.77%, however, these samples are still within the acceptable limit with only one failed point out of 31.

AAPM TG-119 publication recommended that a test is considered successful when more than 90% of the points of γ passing rate, % gamma index of the measured plan agree with the calculated ones, using the criteria of 3%/3 mm (Ezzell *et al.* 2009). The widely recognised gamma index criteria of 3%/3 mm as compared to 3%/2 mm differ in their spatial tolerance, with the 2 mm criterion being more stringent. When using 3%/2 mm, the distance-to-agreement requirement is tighter, meaning that the measured and calculated dose distributions must match within a smaller physical distance. This narrower margin makes the gamma evaluation more sensitive to small discrepancies in spatial alignment, especially in regions with high dose gradients such as target edges or near critical organs. As a result, even minor shifts caused by setup variation, or limitations in measurement resolution can lead to a gamma failure. In contrast, the 3%/3 mm criterion allows for a

wider spatial tolerance, capturing more points as passing, even if minor deviations exist. This is why 3%/3 mm is widely accepted as the clinical standard as it provides a balanced approach that maintains sensitivity to errors while accommodating practical uncertainties in dose delivery and measurement. Therefore, using the 2 mm distance-to-agreement typically results in a higher rate of discrepancy not because the plan is clinically unacceptable, but because the evaluation is stricter and more sensitive to small variations that may not be clinically significant.

Table 4. Gamma Index Comparison for Each Phantom Material with Water

Sample	Total points	Points passed	Points failed	Pass (%)
B	31	31	0	100.00
C	31	31	0	100.00
D	31	31	0	100.00
E	31	31	0	100.00
F	31	31	0	100.00
G	31	30	1	96.77
H	31	30	1	96.77
I	31	31	0	100.00
L	31	31	0	100.00
M	31	30	1	96.77
N	31	30	1	96.77
O	31	31	0	100.00
P	31	30	1	96.77
Q	31	31	0	100.00
R	31	31	0	100.00

Various factors may lead to the impurities of the composition of phantom G, H, M, N and P, which lead to the disparities in the percentage depth dose comparison with water. The process to obtain the elemental composition of the phantom material may be one of the factors contributing to the addition of impurities in the phantom's composition. In energy dispersive X-Ray (EDX) composition analysis, the sample is often coated with gold or platinum to allow better conductivity, allowing the addition of unrelated metal element in the composition. However, previous study reported an analysis of EDX without coating; thus, there is indeed potential in which coating is not required for the measurement of elemental composition (Li *et al.* 2010). However, whether a coating is required depends on the sample itself, and the properties that need to be attained. The disparities also may be attributed by the absence of relevant parameters that may contribute to the contamination or attenuation of the photons reaching the phantom, especially when it comes to simulation study.

These slight deviations in gamma index performance, although still within clinically acceptable thresholds, highlight the importance of rigorous material characterisation and consistency in phantom fabrication. For instance, the presence of residual moisture, variation in binder concentration in sample H, M, N, and P (S. Zuber *et al.* 2021), or uneven distribution of lignocellulosic components may influence the mass density. Changes in composition (Marashdeh *et al.* 2015) and molecular structure of the phantom material may lead to changes in the electron density and effective atomic number, thus altering photon interactions at specific depths. For sample N and P, the composition includes soy protein isolate, distilled water, sodium hydroxide and different percentages of itaconic acid polyamidoamine-epichlorohydrin (5 and 15%). Despite previous literature

reporting that the treatment of sodium hydroxide (NaOH)/itaconic acid polyamidoamine-epichlorohydrin (IA-PAE) with SPI (Samson *et al.* 2020) resulted in high strength with low viscosity, non-toxicity, and high water-resistance, characteristics that prevent delamination and excellent temperature stability, the sample may still exhibit spatial variations in radiation interaction characteristics due to its complexities.

Furthermore, simulation parameters such as voxel size (Goodall and Ebert 2020) or physics models used in GATE, might have compounded the discrepancies observed. The findings of this previous work indicate that adjustments to the dose voxel size have a more significant impact on the displayed dose distribution than changes to statistical uncertainty. Therefore, reducing dose voxel size settings should take precedence over altering statistical uncertainty. In cases where lower dose voxel size settings led to excessive computation times, a minimal increase in dose voxel size should be considered to balance accuracy and computational efficiency. This supports the hypothesis that simulation parameters, particularly voxel size, may influence dose accuracy and contribute to discrepancies. However, these effects remain dependent on the reference voxel size used in the treatment planning system.

CONCLUSIONS

1. A range of plastic and wood-based phantom materials were evaluated for their percentage depth dose using Monte Carlo simulations *via* the Geant4 Application for Emission Tomography (GATE), with gamma index analyses performed for all samples.
2. The percentage depth doses for all the phantom materials pass the 3%/2 mm comparison by gamma index at 96.8%.
3. Percentage depth dose is one of the most vital dosimetric properties especially in radiotherapy treatment planning and findings from this work demonstrate the potential of wood-based phantom material in radiotherapy and medical physics application.

ACKNOWLEDGMENTS

The authors acknowledge the Fundamental Research Grant Scheme (FRGS/1/2024/STG07/UKM/02/4) from the Ministry of Higher Education (MOHE) and Universiti Kebangsaan Malaysia Geran Galakan Penyelidik Muda (GGPM-2023-027).

REFERENCES CITED

Abd Hamid, P. N. K., Yusof, M. F. M., Hashim, R., and Zainon, R. (2018). "Design and evaluation of corn starch-bonded *Rhizophora* spp. particleboard phantoms for SPECT/CT imaging," *IOP Conference Series: Materials Science and Engineering* 298, article 012041. DOI: 10.1088/1757-899X/298/1/012041

Abuarra, A., Hashim, R., Bauk, S., Kandaiya, S., and Tousi, E. T. (2014). "Fabrication and characterization of gum Arabic bonded *Rhizophora* spp. particleboards," *Mater. Des.* 60, 108-115.

Aitelcadi, Z., Bannan, A., Baydaoui, R. El, Mesradi, M. R., and Halimi, A. (2020).

"Feasibility of external radiotherapy dose estimation in homogenous phantom using Monte Carlo modeling," *J. Theor. Appl. Inf. Technol*. 98, 1151-1162.

Allahverdi, M., Nisbet, A., and Thwaites, D. I. (1999). "An evaluation of epoxy resin phantom materials for megavoltage photon dosimetry," *Phys. Med. Biol.* 44, article 1125.

binti Zuber, S. H., Hadi, M. F. R. A., Hashikin, N. A. A., Yusof, M. F. M., and Aziz, M. Z. A. (2024). "Rhizophora-based particleboard bonded with soy flour and lignin as potential phantom," *BioResources* 19, 5467-5482.

Borcia, C., and Mihailescu, D. (2007). "Are water equivalent materials used in electron beams dosimetry really water equivalent?," *Rom. J. Phys.* 53.

Bradley, D. A., Tajuddin, A. A., Sudin, C. W. A. C. W., and Bauk, S. (1991). "Photon attenuation studies on tropical hardwoods," *Int. J. Radiat. Appl. Instrumentation. Part A. Appl. Radiat. Isot.* 42, 771-773.

Breslin, T., Paino, J., Wegner, M., Engels, E., Fiedler, S., Forrester, H., Rennau, H., Bustillo, J., Cameron, M., Häusermann, D., *et al*. (2023). "A novel anthropomorphic phantom composed of tissue-equivalent materials for use in experimental radiotherapy: Design, dosimetry and biological pilot study," *Biomimetics* 8(2), article 230. DOI: 10.3390/biomimetics8020230

Ezzell, G. A., Burmeister, J. W., Dogan, N., LoSasso, T. J., Mechalakos, J. G., Mihailidis, D., Molineu, A., Palta, J. R., Ramsey, C. R., and Salter, B. J. (2009). "IMRT commissioning: Multiple institution planning and dosimetry comparisons, a report from AAPM Task Group 119," *Med. Phys.* 36, 5359-5373.

Goodall, S. K., and Ebert, M. A. (2020). "Recommended dose voxel size and statistical uncertainty parameters for precision of Monte Carlo dose calculation in stereotactic radiotherapy," *J. Appl. Clin. Med. Phys.* 21, 120-130. DOI: 10.1002/acm2.13077

International Atomic Energy Agency (IAEA) (2000). *Absorbed Dose Determination in External Beam Radiotherapy: An International Code of Practice for Dosimetry Based on Standards of Absorbed Dose to Water (Technical Reports Series No. 398)*, Vienna.

Jan, S., Benoit, D., Becheva, E., Carlier, T., Cassol, F., Descourt, P., Frisson, T., Grevillot, L., Guigues, L., Maigne, L., *et al*. (2011). "GATE V6: A major enhancement of the GATE simulation platform enabling modelling of CT and radiotherapy," *Phys. Med. Biol.* 56, 881-901. DOI: 10.1088/0031-9155/56/4/001

Jan, S., Santin, G., Strul, D., Staelens, S., Assié, K., Autret, D., Avner, S., Barbier, R., Bardiès, M., Bloomfield, P. M., *et al*. (2004). "GATE: A simulation toolkit for PET and SPECT," *Phys. Med. Biol.* 49, 4543-4561. DOI: 10.1088/0031-9155/49/19/007

Jusufbegović, M., Pandžić, A., Busuladžić, M., Čiva, L.M., Gazibegović-Busuladžić, A., Šehić, A., Vegar-Zubović, S., Jašić, R., and Beganović, A. (2023). "Utilisation of 3D printing in the manufacturing of an anthropomorphic paediatric head phantom for the optimisation of scanning parameters in CT," *Diagnostics* 13(2), article 328. DOI: 10.3390/diagnostics13020328

Kairn, T., Jessen, L., Bodnar, J., Charles, P. H., and Crowe, S. B. (2023). "Lung radiotherapy verification with a 3D printed thorax phantom and an ionisation chamber array," in: *Journal of Physics: Conference Series*. IOP Publishing, p. 12028.

Li, J., Qian, X., Chen, J., Ding, C., and An, X. (2010). "Conductivity decay of cellulose-polypyrrole conductive paper composite prepared by in situ polymerization method," *Carbohydr. Polym.* 82, 504-509. DOI: 10.1016/j.carbpol.2010.05.036

Lin, B. Z. H., Zhang, E. T., Ng, H., Tan, M. Y. L., Soh, Z. H., Wong, Y. M., Chua, C. G. A., Lew, K. S., Pang, E. P. P., Tan, H. Q., Park, S. Y., Ng, B. F., and Koh, W. Y. C.

(2025). "Design and additive manufacture of patient-specific head phantom for radiotherapy," *Mater. Des.* 252, article 113719. DOI: 10.1016/j.matdes.2025.113719

Marashdeh, M. W., Al-Hamarneh, I. F., Munem, E. M. A., Tajuddin, A. A., Ariffin, A., and Al-Omari, S. (2015). "Determining the mass attenuation coefficient, effective atomic number, and electron density of raw wood and binderless particleboards of *Rhizophora* spp. by using Monte Carlo simulation," *Results Phys.* 5, 228-234.

Rit, S., Pinho, R., Delmon, V., Pech, M., Bouilhol, G., Schaerer, J., Navalpakkam, B., Vandemeulebroucke, J., Seroul, P., Sarrut, D. (2011). "VV, a 4D slicer," in: *Fourth International Workshop on Pulmonary Image Analysis*, Toronto, pp. 171-175.

Samson, D. O., Aziz, M. Z. A., Shukri, A., Jafri, M. Z. M., Hashim, R., Zuber, S. H., Hashikin, N. A. A., Rabba, J. A., Samson, P. A., and Yusof, M. F. M. (2023). "Radiological and dosimetric evaluation of biomaterial composite phantoms with high energy photons and electrons," *Health Phys.* 10-1097.

Samson, D. O., Shukri, A., Jafri, M. Z. M., Hashim, R., Sulaiman, O., Aziz, M. Z. A., and Yusof, M. F. M. (2020). "Characterization of *Rhizophora* SPP. particleboards with SOY protein isolate modified with NaOH/IA-PAE adhesive for use as phantom material at photon energies of 16.59-25.26 keV," *Nucl. Eng. Technol.*

Sarrut, D., Arbor, N., Baudier, T., Borys, D., Etxebeste, A., Fuchs, H., Gajewski, J., Grevillot, L., Jan, S., Kagadis, G.C., *et al*. (2022). "The OpenGATE ecosystem for Monte Carlo simulation in medical physics," *Phys. Med. Biol.* 67. DOI: 10.1088/1361-6560/ac8c83

Sechopoulos, I., Rogers, D. W. O., Bazalova-Carter, M., Bolch, W. E., Heath, E. C., McNitt-Gray, M. F., Sempau, J., and Williamson, J. F. (2018). "RECORDS: Improved reporting of montE CarlO RaDiation transport studies: Report of the AAPM Research Committee Task Group 268," *Med. Phys.* 45, article 12702, e1-e5. DOI: 10.1002/mp.12702

Seco, J., and Evans, P.M. (2006). "Assessing the effect of electron density in photon dose calculations," *Med. Phys.* 33, 540-552. DOI: 10.1118/1.2161407

Taylor, M., Franich, R., Johnston, P., Millar, R., and Trapp, J. (2007). "Systematic variations in polymer gel dosimeter calibration due to container influence and deviations from water equivalence," *Phys. Med. Biol.* 52, 3991-4005. DOI: 10.1088/0031-9155/52/13/022

Yadav, N., Singh, M., Mishra, S.P., and Ansari, S. (2023). "Development of an anthropomorphic heterogeneous female pelvic phantom and its comparison with a homogeneous phantom in advance radiation therapy: Dosimetry analysis," *Med. Sci.* DOI: 10.3390/medsci11030059

Yohannes, I., Kolditz, D., Langner, O., and Kalender, W.A. (2012). "A formulation of tissue-and water-equivalent materials using the stoichiometric analysis method for CT-number calibration in radiotherapy treatment planning," *Phys. Med. Biol.* 57, article 1173.

Yusof, M. F. M., Hamid, P. N. K. A., Tajuddin, A. A., Hashim, R., Bauk, S., Isa, N. M., and Isa, M. J. M. (2017). "Mass attenuation coefficient of tannin-added *Rhizophora* spp. particleboards at 16.59-25.56 keV photons, and 137 Cs and 60 Co gamma energies," *Radiol. Phys. Technol.* 10, 331-339.

Zuber, S., Hashikin, N., Yusof, M .F. M., Aziz, M. Z. A., and Hashim, R. (2021). "Influence of different percentages of binders on the physico-mechanical properties of *Rhizophora* spp. particleboard as natural-based tissue-equivalent phantom for radiation dosimetry applications," *Polymers* (Basel) 13(11), article 1868. DOI: 10.3390/polym13111868

Zuber, S. H., Hashikin, N. A. A., Mohd Yusof, M. F., Aziz, M. Z. A., and Hashim, R. (2021a). "Characterization of soy-lignin bonded *Rhizophora* spp. particleboard as substitute phantom material for radiation dosimetric studies - Investigation of CT number, mass attenuation coefficient and effective atomic number," *Appl. Radiat. Isot.* 170, article 109601. DOI: 10.1016/j.apradiso.2021.109601

Zuber, S. H., Yusof, M. F. M., Hashikin, N. A. A., Samson, D. O., Aziz, M. Z. A., and Hashim, R. (2021b). "*Rhizophora* spp. as potential phantom material in medical physics applications – A review," *Radiat. Phys. Chem.* 189, article 109731. DOI: 10.1016/j.radphyschem.2021.109731

Article submitted: May 20, 2025; Peer review completed: September 27, 2025; Revised version received and accepted: October 12, 2025; Published: October 29, 2025.
DOI: 10.15376/biores.20.4.10858-10871